Improving carbon dioxide capture in aqueous ammonia solutions by fine SiO_2 particles

Donata Konopacka-Łyskawa[1]* (iD) , Temesgen Abeto Amibo[1,2] (iD) , Dominik Dobrzyniewski[1] (iD) ,
Marcin Łapiński[3] (iD)

[1] Gdańsk University of Technology, Faculty of Chemistry, Department of Process Engineering and Chemical Technology, Narutowicza 11/12, 80-233 Gdańsk, Poland
[2] School of Chemical Engineering, Jimma Institute of Technology, Jimma University, Jimma, P.O. Box-378, Ethiopia
[3] Gdańsk University of Technology, Faculty of Applied Physics and Mathematics, Institute of Nanotechnology and Materials Engineering, Narutowicza 11/12, 80-233 Gdańsk, Poland

* Corresponding author:
e-mail:
donata.konopacka-lyskawa@pg.edu.pl

Abstract
Ammonia solutions are considered to be effective solvents for carbon dioxide absorption. Despite numerous advantages of these solvents, their high volatility is a significant technical and economic problem. Therefore, in this work, silica particles were used as additives to improve CO_2 absorption and inhibit NH_3 desorption. SiO_2 microparticles and colloidal SiO_2 particles in the concentration range of 0–0.15 wt.% were used in this study. The most favorable mass transport for CO_2 absorption was at the concentration of colloidal particles of 0.05 wt.%. Under these conditions, the enhancement in the number of moles of absorbed CO_2 was above 30%. However, in solvents containing 0.01 wt.% SiO_2 microparticles, the increase in CO_2 absorption was about 20%. At the same time, the addition of SiO_2 particles significantly reduced the escape of ammonia from the solution. The best improvement was obtained when colloidal SiO_2 particles were added, and then NH_3 escape was decreased by about 60%. This unfavorable phenomenon was also inhibited in ammonia solutions containing SiO_2 microparticles at a concentration of 0.01 wt.%.

Keywords
carbon dioxide, CO_2 absorption, ammonia escape, SiO_2 particles, mass transfer

1. INTRODUCTION

Currently, to slow down climate warming is one of the most important challenges facing our civilization. The increase of the temperature of the Earth's atmosphere is caused by excessive emissions of greenhouse gases (GHG). Despite many political declarations, emissions of gases such as carbon dioxide, methane, nitrogen oxides, and fluorinated gases are still growing (with a slight decrease in 2020 due to the COVID-19 pandemic) (Olivier, 2022). Their total emissions expressed as CO_2 equivalent amounted to 49.5 gigatons (IEA, 2022), with the largest share in GHG emissions from industry and the electric power sector. Among the greenhouse gases, CO_2 is the most emitted, which accounts for about 72% (excluding land-use change) of all GHGs (Olivier, 2022). A report prepared in 2022 by the Intergovernmental Panel on Climate Change (Pörtner et al., 2022) indicates that the temperature increase since pre-industrial times is now above $1\,^\circ$C. However, if the concentration of greenhouse gases continues to grow at the same rate, in 2030 the temperature increase will be $1.5\,^\circ$C. And this growth is much faster than assumed in previous forecasts. An increase in the concentration of greenhouse gases will entail irreversible climate changes that will affect the life of our entire planet. Climate warming is expected to affect various aspects of life on Earth, including loss of biodiversity, tree mortality, increase in wildfires,

and transformation in the physiology of organisms involved in the carbon cycle on earth. The changes in ecosystems also affect such areas of our lives as the availability of drinking water, food production, and the intensification of extreme weather events. Therefore, efforts are being made to slow down this upward trend of CO_2 concentrations in the atmosphere. On the one hand, work is aimed at raising public awareness, including promoting a change in lifestyle, e.g., by limiting excessive consumption and everyday pro-ecological activities (e.g. reducing the consumption of plastic packaging, saving water, promoting energy-saving solutions). On the other hand, efforts are being made to develop CO_2 net-zero emission technologies, which are based on the use of renewable energies and the concept of CO_2 capture, utilization and sequestration (CCUS) or CO_2 capture and utilization (CCU).

The proposed carbon dioxide capture methods are most often classified as post-conversion, pre-conversion, and oxy-fuel combustion (Al-Hamed and Dincer, 2021; Cuéllar-Franca and Azapagic, 2015). Post-conversion capture is used to purify the gas stream, e.g. generated after the combustion of fossil fuels, in the production of cement, fuels, steel, or biogas. Pre-conversion methods are used to remove CO_2 formed as an undesirable by-product, e.g. during ammonia production, steam reforming, or coal gasification. However, oxy-fuel combustion refers to processes such as fuel combustion or pro-

duction, where a clean stream of oxygen is used to burn fossil fuels, resulting in a CO_2-rich leaving gas without nitrogen and NO_x impurities. Post-conversion CO_2 capture uses absorption processes, adsorption processes, cryogenic separation, chemical reactions, and membrane processes. Absorption processes in both chemical and physical solvents are indicated as the main options for pre-conversion capture. Whereas oxy-fuel combustion can be carried out as combustion in pure oxygen, using chemical looping or chemical looping reforming (Chao et al., 2021; Cuéllar-Franca and Azapagic, 2015). The solutions proposed in the post-combustion group can be incorporated relatively simply into existing installations that burn fossil fuels. The largest share in CO_2 capture is attributed to processes using physical or chemical absorption (57%) (Chao et al., 2021). Such a wide use of absorption in CO_2 capture is due to the fact that it is a mature process and many companies offer ready-made solutions. Solvents such as dimethyl ether of polyethylene glycols (Selexol), methanol (Rectisol, Ifpexol), propylene carbonate (Fluor) or N-methyl 2-pyrrolidone (Purisol) are used for physical absorption (Ban et al., 2014; Borhani and Wang, 2019). The most popular solvents for chemical absorption are amines, e.g. monoethanolamine (MEA), 2-(2-aminoethoxy) ethanol (DGA), N-methyldiethnolamine (MDEA) and salt solutions, e.g. potassium carbonate (Borhani and Wang, 2019; Chai et al., 2022).

At present, ammonia solutions are also considered promising solvents for chemical absorption (Al-Hamed and Dincer, 2021). Among their advantages are low cost, relatively high stability compared to amine-based solvents, high CO_2 removal capacity, low heat of absorption, and lower energy requirements during regeneration. When ammonia solutions are applied to capture exhaust gases containing nitrogen and sulfur oxides, valuable by-products can be obtained, e.g. ammonium sulfate or ammonium nitrate, which are popular fertilizers (Yang et al., 2014). Despite the numerous advantages of ammonia solutions as an absorbent for CO_2 capture, its high volatility is a significant technical and economic problem. Both during the absorption of CO_2 and in the stripping step, some of the ammonia escapes. On the one hand, this reduces its concentration in the solvent, on the other hand, ammonia reacts with the desorbed carbon dioxide to form solid ammonium carbonate deposited in pipes and valves (Wang et al., 2018).

Various strategies are used to improve the absorption process, e.g. using amine mixture solutions or activators to common solvents, testing new compounds for CO_2 absorption, e.g. ionic liquids or newly synthesized amines, and deep-eutectic solvents (Bińczyk et al., 2019; Chai et al., 2022; Liu et al., 2021; Ochedi et al., 2021). Recently, nanofluids have been proposed as a new type of absorbent (Tavakoli et al., 2022). Nanofluids consist of a base liquid and nanoparticles, and the small size of the added materials affects the high stability of the dispersion produced. The results of absorption studies on nanofluids are promising and indicate that it is possible to increase the absorption rate during both physical and chemical absorption (Tavakoli et al., 2022). From a practical point of view, effective solvents are nanofluids based on chemical absorbents, which are characterized by high absorption capacity. The tested solvents containing amines and nanoparticles showed an increase in the absorption rate of several dozen percent (Tavakoli et al., 2022). Zhang et al. (2020) obtained an enhancement in the rate of CO_2 absorption in ammonia solutions with the addition of Fe_3O_4 nanoparticles, with the most favorable effect observed (increase by 14.5%) for the solution with the highest tested ammonia concentration of 4%. The cost of commercially available nanoparticles is relatively high. Moreover, there have been no literature reports on studies of CO_2 absorption in ammonia solutions containing SiO_2 particles. Therefore, in this work, colloidal SiO_2 with an average diameter of 600 nm was tested as an additive to the absorption solutions. The aim of the conducted research was: (i) to determine the rate of CO_2 absorption in dispersions obtained on the basis of aqueous solutions of ammonia and colloidal SiO_2 particles and in aqueous dispersions containing ammonia and SiO_2 microparticles; (ii) testing the influence of the presence of SiO_2 particles on ammonia desorption during the flow of the gas mixture through the absorber and (iii) determining the most favorable concentration of fine particles in ammonia solutions for carbon dioxide capture.

2. EXPERIMENTAL

25% ammonia solution ($\geq$ 96.0%; POCH, Poland), silicon oxide ($>$ CIECH, Poland), colloidal silica Aerosil® 200 ($>$ 99.8%, Evonik, Germany), gum arabic from acacia tree (Sigma-Aldrich, Germany), CO_2 gas (Oxygen s.c., Poland) were used without further purification. The water used to prepare all solutions was obtained by reverse osmosis.

Measurements of CO_2 absorption were performed in a bubble reactor. The flow rate of CO_2 and air was regulated by mass flow controllers. The gas mixture was introduced into the ammonia solution through a glass sinter, and the CO_2 and NH_3 content in the exhaust gas was analyzed using sensors and recorded in a computer. A detailed description of the tested setup was published elsewhere (Czaplicka et al., 2022).

Aqueous solutions of ammonia with NH_3 concentration of 0.53 mol·dm^{-3} containing SiO_2 from 0 to 0.15 wt.% in the form of colloidal or microparticles were used as solvents for CO_2 absorption. To obtain a stable dispersion during measurements, the initial suspension of SiO_2 particles in water with the addition of gum arabic (100 ppm) as a dispersion stabilizer was prepared and sonicated in an ultrasonic bath for 30 minutes. Then the right amount of commercial ammonia solution and the rest of the water were added to obtain the assumed concentrations of ammonia in the tested solvent. The volume of the tested absorbent was 0.250 dm^3, and the volume flow rate of the CO_2-air gas mixture ($x_{V,CO2} = 0.15$)

was 0.5 dm$^3 \cdot$min^{-1} in each experiment. CO_2 absorption in a tested solvent was carried out for 30 min. Stability of SiO_2 dispersions was controlled with the sedimentation method. For this purpose, the freshly prepared SiO_2 dispersion in the ammonia solution was placed in the vessel and suspension photos were taken after a time of 0, 4 and 24 hours. To characterize the used SiO_2 particles, scanning electron microscope (SEM) equipped with a secondary electron detector (FEI Quanta FEG 250) was used. The size of colloidal SiO_2 was determined using ZETASIZER (Malvern).

3. RESULTS AND DISCUSSION

3.1. Characterization of SiO$_2$ dispersion

Measurements were made in ammonia solutions containing SiO_2 microparticles and colloidal SiO_2 particles. Exemplary images of these particles are shown in Fig. 1. SiO_2 microparticles in the form of aggregates are visible in SEM images, and their size ranges from about 1 μm to about 47 μm. However, the structure of the colloidal particles is not visible in the SEM images. Aerosil® 200 is a colloidal silica consisting of aggregates of nanoparticles. In this case, the size of these aggregates was measured with dynamic light scattering, determining the velocity of particle movement due to Brownian motion. Previously, the samples were sonicated for 30 min, the same time as during the solvent preparation used for the absorption measurements. The mean hydrodynamic particle size obtained was 594 nm.

Figure 2 shows the visualization of the obtained dispersions immediately after their preparation and after 4 and 24 hours. In the stability test, larger SiO_2 particles settled down in the dispersion prepared based on ammonia solutions and microparticles. However, in the case of solutions containing colloidal SiO_2 particles, the obtained dispersions were stable for 24 h. It should be emphasized that during the measurements when gas bubbles flowed through the absorbent and caused mixing of the solvent, both microparticles and colloidal particles remained suspended in the liquid.

3.2. CO$_2$ absorption

The change in CO_2 concentration in the gas outlet stream over time is shown in Fig. 3. The course of CO_2 absorption
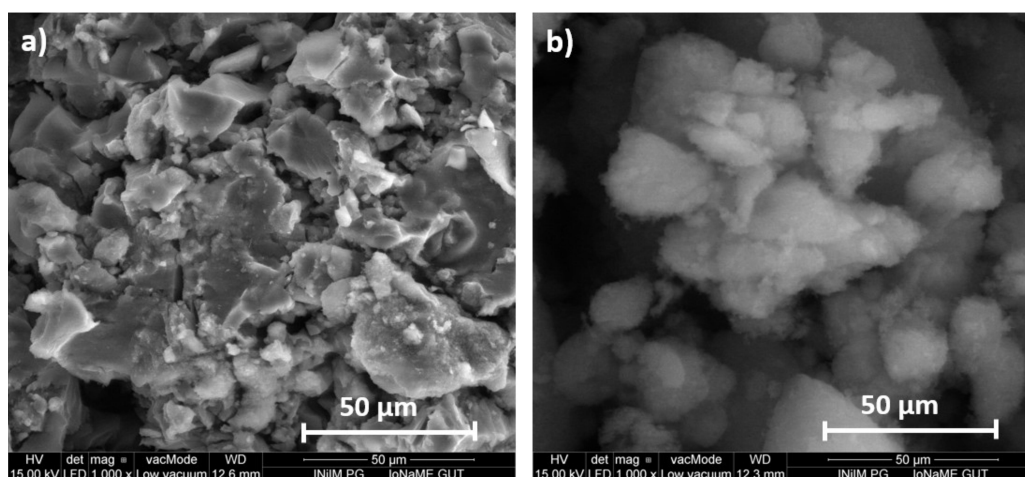

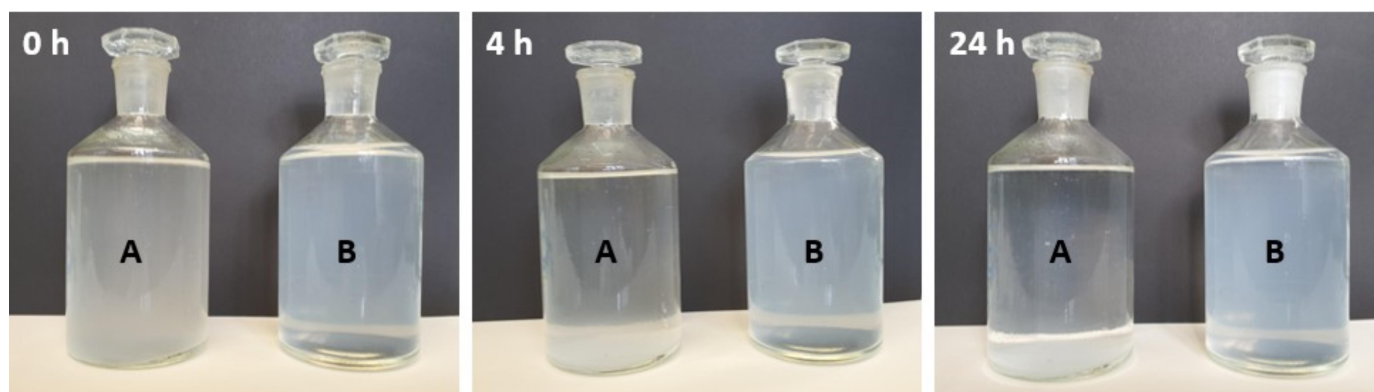Figure 1. SEM images of used SiO2 particles: a) microparticles; b) colloidal particles.

Figure 2. Photographs of prepared dispersions containing SiO_2 microparticles (A) and colloidal SiO_2 particles (B) after 0, 4, and 24 hours.
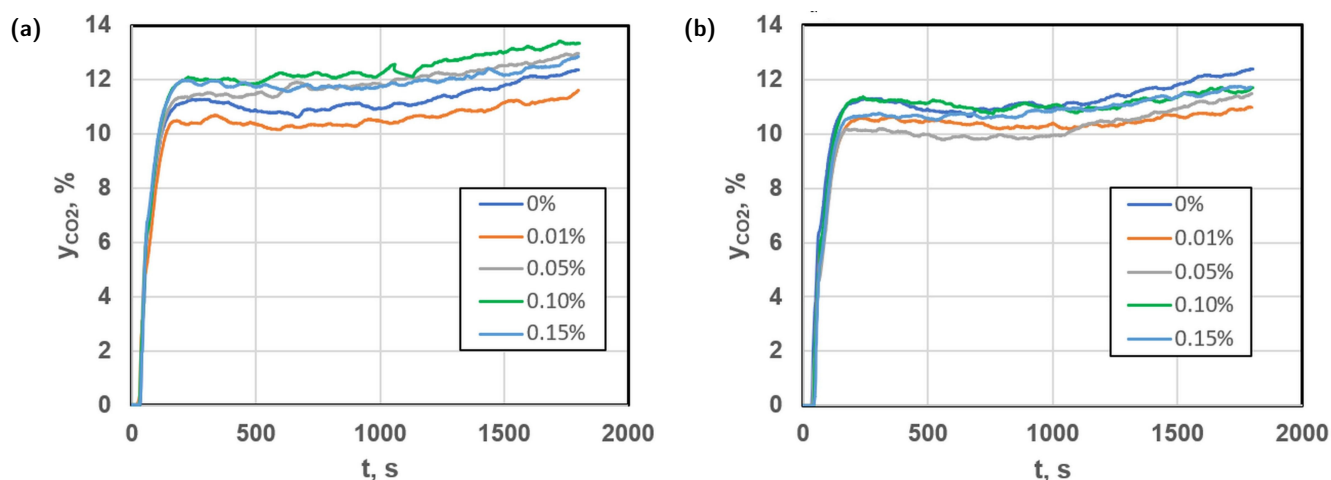
Figure 3. The volume fraction of carbon dioxide in the outlet gas stream for experiments with: a) SiO_2 microparticles; b) colloidal SiO_2 particles.

in the tested system can be divided into three periods. In the initial period, just after the start of measurements, there was no CO_2 in the outlet gas which may be related to the capture of all supplied CO_2 in the ammonia solution. Then, the concentration of CO_2 in the gas outlet stream increased rapidly, and the conditions of the absorption process were established. Next, stable carbon dioxide capture was observed, and changes in CO_2 concentration were not significant. During the second period, the pH of the solvent was relatively high, which favored the uptake of CO_2. After about 1000 s, a gradual increase in CO_2 was observed in all experiments. The reduction of the CO_2 absorption rate can result from a decrease of the pH due to the reaction of forming carbonate anions with ammonium cations in the solution. Comparing the changes in the molar fraction of CO_2 in the gas outlet during absorption in solvents containing SiO_2 microparticles and in solvents with colloidal particles, the CO_2 concentration in the outlet gas was lower when dispersions of colloidal particles were used as absorbents.

Based on the known air stream introduced into the absorber and the concentration of CO_2 in the inlet and outlet streams, the total number of moles of CO_2 captured during the absorption was determined. The molar flux of absorbed CO_2 can be determined as:

$$Q_{CO2} = Q_{air} \left(Y_{in}^{CO2} - Y_{out}^{CO2} \right) \qquad (1)$$

where Q_{air} is the mole flux of air, Y_{in}^{CO2} and Y_{out}^{CO2} are relative mole fractions of carbon dioxide in the inlet and outlet gas.

Figure 4 shows the dependence of the number of moles of captured CO_2 on the concentration of SiO_2 particles in the ammonia solution. The greatest amount of CO_2 was absorbed in the dispersion containing 0.05 wt.% of colloidal silica within 30 minutes. These results reflect the observed changes of CO_2 concentration in the exhaust gas during absorption in the tested dispersions.
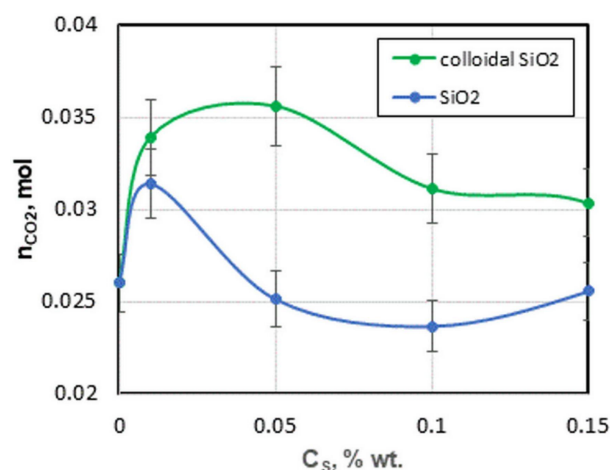

Figure 4. Influence of the concentration of SiO_2 particles on the number of moles of carbon dioxide captured.

The molar flow rate of carbon dioxide N_{CO2} transported from gas into the liquid phase can be expressed as:

$$N_{CO2} = K_G \left(p_G^{CO2} - p_L^{CO2} \right) \qquad (2)$$

where K_G is the overall mass transfer coefficient of carbon dioxide, p_G^{CO2} and p_L^{CO2} are partial pressures in the gas phase and liquid phase, respectively.

The partial pressure of CO_2 in the gas phase was estimated using the logarithmic mean values of CO_2 molar fraction (Ma et al., 2016):

$$p_G^{CO2} = P \frac{y_{in}^{CO2} - y_{out}^{CO2}}{\ln \frac{y_{in}^{CO2}}{y_{out}^{CO2}}} \qquad (3)$$

and the partial pressure of CO_2 in a liquid phase depends on the concentration of free CO_2 in the liquid phase C_L^{CO2} and the Henry's constant H_L^{CO2}:

$$p_L^{CO2} = C_L^{CO2} H_L^{CO2} \qquad (4)$$

Henry's constant for CO_2 in ammonia solution was calculated using "NO_2 analogy" (Atzori et al., 2023) as:

$$H_L^{CO2} = H_L^{NO2} \left(\frac{H_w^{CO2}}{H_w^{NO2}} \right) \qquad (5)$$

Correlations used for the calculations of the Henry's constants as functions of temperature are listed in Table 1.

The concentration of free CO_2 in the ammonia solution was determined on the basis of the current concentration of CO_2 (as the number of moles of CO_2 absorbed in a known volume of the solution), dissociation constants of carbonic acid and water listed in Table 2, and pH of the solution. Similarly, the concentration of free NH_3 needed to evaluate Henry's constant for N_2O in an ammonia solution was determined. The current concentration of ammonia in the solution, the dissociation constants of ammonia and water calculated according to the correlations presented in Table 2, and the pH of the solution were used to calculate free ammonia in the solution.

Using the molar flow rate of CO_2 calculated as:

$$N_{CO2} = \frac{Q_{CO2}}{A} = \frac{Q_{CO2}}{aV_L} \qquad (6)$$

where A is the gas-liquid interface area, a is a specific surface area (in the unit solution volume), and V_L is the volume of solution used in the experiment, and combining equations (1)–(6), the overall volumetric mass transfer coefficients of CO_2 absorption $K_G a$ were determined. The values are summarized in Table 3. The obtained $K_G a$ values are comparable to the results calculated by Ma et al. (2016), where $K_G a = 3.03 \cdot 10^{-5}$ mol·m^{-3}·s^{-1}·Pa^{-1} determined at the temperature of $20\,°C$ in the ammonia solution at a concentration of 0.625 mol·dm^{-3} when the mole fraction of CO_2 in the gas inlet stream was equal to 15%. Higher $K_G a$ values were obtained for solvents containing colloidal SiO_2 particles. The most favorable mass transport conditions were when the concentration of colloidal particles was 0.05 wt.%. However, the improvement of CO_2 mass transfer in solvents containing SiO_2 microparticles occurred for the lowest concentration used, i.e. 0.01 wt.%. The addition of microparticles in the amount of 0.05 wt.% and higher resulted in a decrease of the CO_2 absorption rate. This is consistent with the previously discussed results of the amount of CO_2 moles adsorbed in the solvent.

3.3. Release of ammonia during CO_2 capture

The courses of ammonia concentration in outlet gas over time are shown in Fig. 5. Three stages can be distinguished during measurements. The first period is the shortest and characterized by a small maximum occurring about 40 s from the start of absorption. It is correlated with the full capture of CO_2 in this stage. Then the ammonia is relatively easily

Table 1. Henry's constants.

System	Henry's constant [Pa·m^3·mol^{-1}]	Ref.
CO_2 − water	$H_w^{CO2} = \frac{10^4}{3.4} \exp\left[-2400 \left(\frac{1}{T} - \frac{1}{298.15} \right) \right]$	Sander (2015)
NO_2 − water	$H_w^{NO2} = \frac{10^5}{1.9} \exp\left[-1400 \left(\frac{1}{T} - \frac{1}{298.15} \right) \right]$	Sander (2015)
NO_2 − NH_3 solution	$H_L^{NO2} = \left(0.155 + 8.17 \cdot 10^{-3} \cdot C_L^{NH3} \right) \cdot 10^6 \exp\left(-\frac{0.00115}{T} \right)$	Seo et al. (2011)
NH_3 − water	$H_w^{NH3} = \frac{1}{0.59} \exp\left[-4200 \left(\frac{1}{T} - \frac{1}{298.15} \right) \right]$	Sander (2015)

Table 2. Dissociation constants (Atzori et al., 2023).

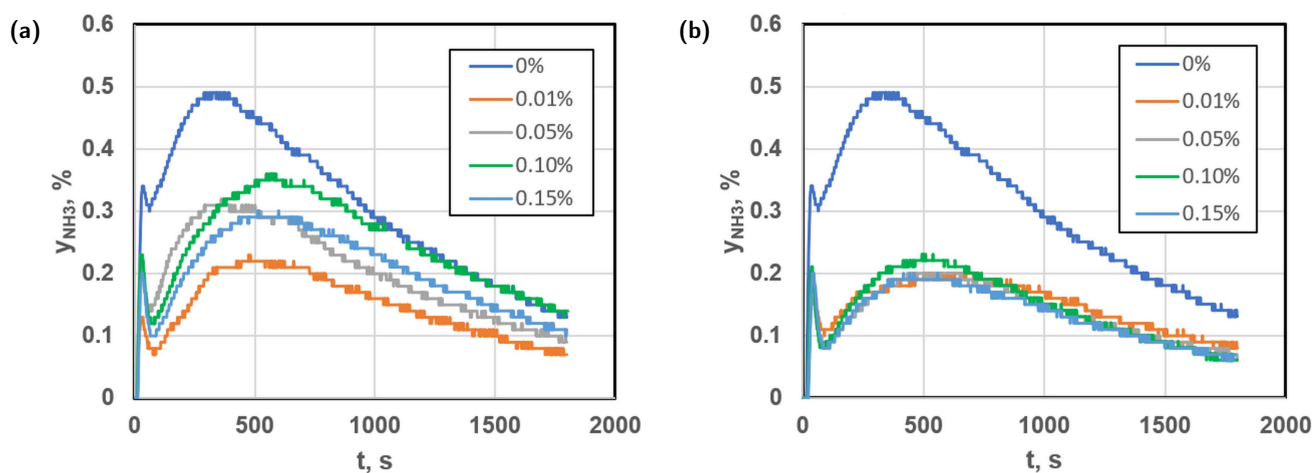| Reaction	Dissociation constant
$H_2O \leftrightarrow OH^- + H^+$	$\lg K_w = -3.981 \frac{10^7}{T^3} + \frac{223620}{T^2} - \frac{3245.2}{T} - 4.098$
$CO_2 + H_2O \leftrightarrow HCO_3^- + H^+$	$\lg K_{a1} = -\frac{3404.71}{T} + 14.8435 - 0.032786T$
$HCO_3^- \leftrightarrow CO_3^{2-} + H^+$	$\lg K_{a2} = -\frac{2909.1}{T} + 6.119 - 0.02272T$
$NH_3 + H_2O \leftrightarrow NH_4^+ + OH^-$	$\ln K_{am} = -\frac{3335.7}{T} - 1.257 - 0.037057T + 1.497 \log T$

Figure 5. The volume fraction of ammonia in the outlet gas stream for selected experiments with: a) SiO_2 microparticles; b) colloidal SiO_2 particles.

Table 3. The effect of particle concentration on the overall volumetric mass transfer coefficient of carbon dioxide absorption.

C_S [wt.%]	$K_G a \cdot 10^5$ [mol·m^{-3}·s^{-1}·Pa^{-1}]	
	SiO_2 microparticles	colloidal SiO_2
0	3.42	
0.01	4.32	4.81
0.05	3.31	5.10
0.1	2.92	4.64
0.15	3.29	4.18

desorbed because the NH_3 dissociation shifts the equilibrium towards the formation of free ammonia in solutions of high pH solution at the beginning of the process. Next, in the second period, NH_3 concentration rises to reach the main maximum concentration. The highest share of ammonia in the outlet gas is for the NH_3 solution without adding SiO_2 particles after about 350 s. A similar value of ammonia concentration in the gas outlet stream was obtained by Ma et al. (2016), who conducted experiments in similar conditions. In suspensions, ammonia desorption is slower and the NH_3 maximum appears after a longer measurement time. The last period is characterized by a decrease in ammonia concentration in outlet gas because of the lower concentration of free NH_3 in the solution as the pH drops due to CO_2 absorption. Based on the output curves for ammonia, the number of moles of NH_3 escaping from the solvent was determined. Fig. 6 shows these data depending on the concentration of microparticles and colloidal SiO_2 particles. Both the presence of microparticles and colloidal SiO_2 particles significantly reduced ammonia escape. In suspensions prepared with SiO_2 microparticles, the greatest inhibition of NH_3 desorption was for a particle concentration of 0.1 wt.%. However, colloidal SiO_2 particles in solvents acted as a highly effective ammonia escape reduction in the entire tested concentration range.
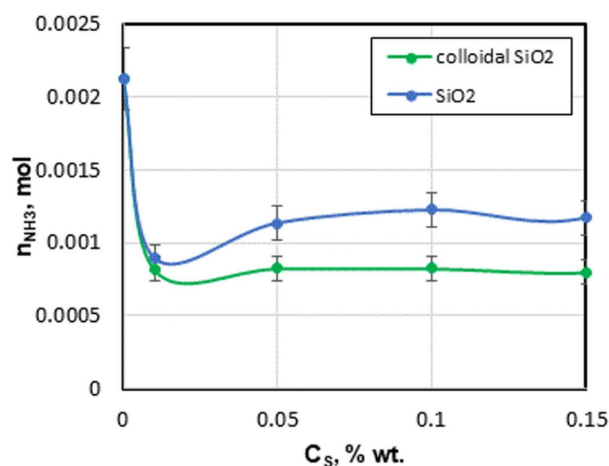

Figure 6. Influence of the concentration of SiO_2 particles on the number of moles of ammonia desorbed.

The NH_3 molar flux was calculated from the equation:

$$N_{NH3} = \frac{Q_{NH3}}{A} = \frac{\left(Y_{out}^{NH3} - Y_{in}^{NH3}\right) Q_{air}}{a V_L} \qquad (7)$$

where Q_{NH3} is the molar flow rate of ammonia, Q_{air} is the molar flow rate of air, Y_{out}^{NH3} and Y_{in}^{NH3} are relative molar fractions of ammonia in the outlet and inlet gas streams, A is the gas-liquid interface area, a is the specific surface area (in the unit solution volume), and V_L is the volume of solution used in the experiment.

The molar flux of ammonia in the gas is the result of its transfer from the solution into the gas phase can be expressed by the relationship:

$$N_{NH3} = K_L \left(C_L^{NH3} - C^{NH3*}\right) \qquad (8)$$

where K_L is the overall mass transfer coefficient in a liquid phase, C_L^{NH3} is the concentration of free ammonia in the solution and C^{NH3*} is the equilibrium concentration of ammonia

with the respect to its content in the gas phase. The concentration of free ammonia in the solution was determined based on the dissociation constant of ammonia and the pH value of the solution, while the equilibrium ammonia concentration was calculated from the Henry's law using the mean partial pressure of ammonia in a gas phase (Ma et al., 2016):

$$C^{NH3*} = \frac{\left(y_{in}^{NH3} + y_{out}^{NH3}\right)}{2} \frac{P}{H_{NH3}} \qquad (9)$$

Combining Equations (7)–(9), the overall volumetric mass transfer coefficient $K_L a$ of ammonia escape was determined and the obtained $K_L a$ values are collected in Table 4.

Table 4. The effect of particle concentration on the overall volumetric mass transfer coefficient of ammonia desorption.

C_S [wt.%]	$K_L a \cdot 10^5$ [s^{-1}]	
	SiO$_2$ microparticles	colloidal SiO$_2$
0	5.43	
0.01	1.97	1.74
0.05	2.52	1.75
0.1	2.72	1.79
0.15	2.62	1.68

The highest $K_L a$ value was for the NH$_3$ desorption from the ammonia solution, while the addition of SiO$_2$ particles resulted in a reduction of the volumetric mass transfer coefficients. The values of the mass transfer coefficient of ammonia from a solution without SiO$_2$ particles are similar to those obtained for NH$_3$ stripping from its solutions of high pH (Kim et al., 2021; Liu et al., 2015). The effect of silica particle concentration on the mass transfer coefficient is consistent with the determined number of moles of ammonia removed from the solvent during gas flow. The addition of colloidal SiO$_2$ particles in the smallest amount used (0.01 wt.%) reduced ammonia desorption by about three times, and further increasing the concentration did not improve its performance. On the other hand, the presence of SiO$_2$ microparticles results in an approximately two-fold slowdown of NH$_3$ removal from the solution, with the most effective result obtained for the lowest concentration of silica, i.e., 0.01 wt.%.

Comparing the effect of SiO$_2$ particles on promoting CO$_2$ absorption and reducing NH$_3$ escape, it can be seen that used types of silica improve both processes. The explanation for this phenomenon is not evident. Analyzing the data collected in the review paper (Mahmoudi and Hlawitschka, 2022), it can be concluded that the influence of solid particles on mass transfer is ambiguous. This is because fine particles can affect the hydrodynamics of a three-phase system (gas-solid-liquid) by reducing the thickness of the gas-liquid interface, affecting the turbulence of mixing by increasing the rate of renewal of the boundary surface, affecting the coalescence of

gas bubbles and the size of the gas-liquid surface area. Also, the particles can cause a shuttle effect by assisting in the transfer from gas to liquid due to the adsorption of the component on the surface of the solid (Alper et al., 1980). This phenomenon may occur when particles have a large specific surface area. Usually, the values of volumetric mass transfer coefficients decrease with increasing solid concentration (Mahmoudi and Hlawitschka, 2022). This is caused by the reduction of the interfacial area due to the addition of solid particles. It is the dominant effect during mass transfer in a three-phase system (Sauer and Hempel, 1987). On the other hand, the opposite effect was reported in some studies when higher volumetric mass transfer coefficients were determined in the suspension produced with fine solid particles of low concentrations (Chen et al., 2013; Mena et al., 2011). In these systems, the increase of $K_L a$ values was explained based on increased turbulence and interfacial renewal, as well as the presence of small particles on the surface of the bubbles inhibiting their coalescence. It seems that the observed duality in the action of silica particles during CO$_2$ absorption in ammonia solution may also be caused by the fact that ammonia molecules can adsorb on the surface of SiO$_2$ particles (Blomfield and Little, 1973; Kuchyanov et al., 2019). The relatively strong interaction of NH$_3$ molecules with the SiO$_2$ surface may hinder its desorption. At the same time, increased ammonia concentration at the interface may favor the capture of CO$_2$ from the gas phase.

4. CONCLUSIONS

In these studies, the effect of silica microparticles and colloidal silica in ammonia solutions on CO$_2$ absorption and escape of ammonia from the solvent was investigated. It was shown that adding SiO$_2$ particles at a low concentration improved carbon dioxide capture and decreased the desorption of ammonia from the solvent. In particular, colloidal SiO$_2$ particles had a more favorable effect. The calculated enhancement in absorbed CO$_2$ was above 30% in solvents containing 0.01 wt.% and 0.05 wt.% colloidal SiO$_2$. Moreover, the presence of colloidal silica caused a positive effect on the desorption of ammonia and reduced the number of moles of NH$_3$ stripped into the flowing gas by about 60%. The obtained results of research on the use of suspensions of fine particles in SiO$_2$ in ammonia solutions as carbon dioxide absorbents can be used in practice to produce new-generation solvents. In addition, the relatively low price of these particles compared to nanoparticles will not significantly affect the cost of CO$_2$ capture.

SYMBOLS

a specific surface area, m^2/m^3
A gas-liquid interface area, m^2
C molar concentration, mol/m^3

H	Henry's constant, m^3 Pa /mol
K_G	overall mass transfer coefficient in a gas phase, mol/(m^2s·Pa)
$K_G a$	overall volumetric mass transfer coefficient in a gas phase, mol/(m^3s·Pa)
K_L	overall mass transfer coefficient in a liquid phase, m/s
$K_L a$	overall volumetric mass transfer coefficient in liquid phase, 1/s
N	molar flow rate, mol/(m^2s)
p	partial pressure, Pa
P	pressure, Pa
Q	mole flux, mol/s
V_L	volume of liquid phase, mol/(m^2s)
y	mole fraction, mol/mol
Y	relative mole fraction, mol/mol

Superscripts

CO2	carbon dioxide
NH3	ammonia
NO2	nitrogen dioxide

Subscripts

air	air
CO2	carbon dioxide
in	inlet
L	liquid
out	outlet
NH3	ammonia
w	water

REFERENCES

Al-Hamed K.H.M., Dincer I., 2021. A comparative review of potential ammonia-based carbon capture systems. *J. Environ. Manage.*, 287, 112357. DOI: 10.1016/j.jenvman.2021.112357.

Alper E., Wichtendahl B., Deckwer W.-D., 1980. Gas absorption mechanism in catalytic slurry reactors. *Chem. Eng. Sci.*, 35, 217–222. DOI: 10.1016/0009-2509(80)80090-X.

Atzori F., Barzagli F., Varone A., Cao G., Concas A., 2023. CO_2 absorption in aqueous NH_3 solutions: Novel dynamic modeling of experimental outcomes. *Chem. Eng. J.*, 451, 138999. DOI: 10.1016/j.cej.2022.138999.

Ban Z.H., Keong L.K., Mohd Shariff A., 2014. Physical absorption of CO_2 capture: A review. *Adv. Mater. Res.*, 917, 134–143. DOI: 10.4028/www.scientific.net/AMR.917.134.

Bińczyk G., Pohorecki R., Moniuk W., Możeński C., 2019. Amine activators of CO_2 absorption in industrial conditions. *Chem. Process Eng.*, 40, 157–165. DOI: 10.24425/cpe.2019.126108.

Blomfield G.A., Little L.H., 1973. Chemisorption of ammonia on silica. *Can. J. Chem.*, 51, 1771–1781. DOI: 10.1139/v73-265.

Borhani T.N., Wang M., 2019. Role of solvents in CO_2 capture processes: The review of selection and design methods. *Renewable Sustainable Energy Rev.*, 114, 109299. DOI: 10.1016/j.rser.2019.109299.

Chai S.Y.W., Ngu L.H., How B.S., 2022. Review of carbon capture absorbents for CO_2 utilization. *Greenhouse Gas. Sci. Technol.*, 12, 394–427. DOI: 10.1002/ghg.2151.

Chao C., Deng Y., Dewil R., Baeyens J., Fan X., 2021. Post-combustion carbon capture. *Renewable Sustainable Energy Rev.*, 138, 110490. DOI: 10.1016/j.rser.2020.110490.

Chen Z., Liu H., Zhang H., Ying W., Fang D., 2013. Oxygen mass transfer coefficient in bubble column slurry reactor with ultrafine suspended particles and neural network prediction. *Can. J. Chem. Eng.*, 91, 532–541. DOI: 10.1002/cjce.21663.

Cuéllar-Franca R.M., Azapagic A., 2015. Carbon capture, storage and utilisation technologies: A critical analysis and comparison of their life cycle environmental impacts. *J. CO2 Util.*, 9, 82–102. DOI: 10.1016/j.jcou.2014.12.001.

Czaplicka N., Dobrzyniewski D., Dudziak S., Jiang C., Konopacka-Łyskawa D., 2022. Improvement of CO_2 absorption and inhibition of NH_3 escape during $CaCO_3$ precipitation in the presence of selected alcohols and polyols. *J. CO2 Util.*, 62, 102085. DOI: 10.1016/j.jcou.2022.102085.

IEA, 2022. *Global energy review: CO₂ emissions in 2021*. International Energy Agency. Available at: https://www.iea.org/reports/global-energy-review-co2-emissions-in-2021-2

Kim E.J., Kim H., Lee E., 2021. Influence of ammonia stripping parameters on the efficiency and mass transfer rate of ammonia removal. *Appl. Sci.*, 11, 441. DOI: 10.3390/app11010441.

Kuchyanov A.S., Chubakov P.A., Chubakov V.P., Mikerin S.L., 2019. Nonlinear interaction of silica photonic crystals with ammonia vapor. *Results Phys.*, 15, 102726. DOI: 10.1016/j.rinp.2019.102726.

Liu B., Giannis A., Zhang J., Chang V.W.-C., Wang J.-Y., 2015. Air stripping process for ammonia recovery from source-separated urine: modeling and optimization. *J. Chem. Technol. Biotechnol.*, 90, 2208–2217. DOI: 10.1002/jctb.4535.

Liu Y., Dai Z., Zhang Z., Zeng S., Li F., Zhang X., Nie Y., Zhang L., Zhang S., Ji X., 2021. Ionic liquids/deep eutectic solvents for CO_2 capture: Reviewing and evaluating. *Green Energy Environ.* 6, 314–328. DOI: 10.1016/j.gee.2020.11.024.

Ma S., Chen G., Zhu S., Han T., Yu W., 2016. Mass transfer of ammonia escape and CO_2 absorption in CO_2 capture using ammonia solution in bubbling reactor. *Appl. Energy*, 162, 354–362. DOI: 10.1016/j.apenergy.2015.10.089.

Mahmoudi S., Hlawitschka M.W., 2022. Effect of solid particles on the slurry bubble columns behavior – A review. *ChemBioEng Rev.*, 9, 63–92. DOI: 10.1002/cben.202100032.

Mena P., Ferreira A., Teixeira J.A., Rocha F., 2011. Effect of some solid properties on gas–liquid mass transfer in a bubble column. *Chem. Eng. Process. Process Intensif.*, 50, 181–188. DOI: 10.1016/j.cep.2010.12.013.

Ochedi F.O., Yu J., Yu H., Liu Y., Hussain A., 2021. Carbon dioxide capture using liquid absorption methods: a review. *Environ. Chem. Lett.*, 19, 77–109. DOI: 10.1007/s10311-020-01093-8.

Olivier J.G.J., 2022. Trends in global CO_2 and total greenhouse gas emissions. 2021 Summary Report. PBL Netherlands Environmental Assessment Agency, The Hague. Available at: https://www.pbl.nl/en/trends-in-global-co2-emissions.

Pörtner H.O., Roberts D.C., Poloczanska E.S., Mintenbeck K., Tignor M., Alegría A., Craig M., Langsdorf S., Löschke S., Möller V., Okem A., 2022. *Climate change 2022: Impacts, adaptation and vulnerability. Summary for policymakers, Technical summary and full report*. IPCC, Switzerland. Available at: https://www.ipcc.ch/report/sixth-assessment-report-working-group-ii/.

Sander R., 2015. Compilation of Henry's law constants (version 4.0) for water as solvent. *Atmos. Chem. Phys.*, 15, 4399–4981. DOI: 10.5194/acp-15-4399-2015.

Sauer T., Hempel D.-C., 1987. Fluid dynamics and mass transfer in a bubble column with suspended particles. *Chem. Eng. Technol.*, 10, 180–189. DOI: 10.1002/ceat.270100123.

Seo J.-B., Jeon S.-B., Lee S.-S., Kim J.-Y., Oh K.-J., 2011. The physical solubilities and diffusivities of N$_2$O and CO$_2$ in aqueous ammonia solutions on the additions of AMP, glycerol and ethylene glycol. *Korean J. Chem. Eng.*, 28, 1698–1705. DOI: 10.1007/s11814-011-0030-8.

Tavakoli A., Rahimi K., Saghandali F., Scott J., Lovell E., 2022. Nanofluid preparation, stability and performance for CO$_2$ absorption and desorption enhancement: A review. *J. Environ. Manage.*, 313, 114955. DOI: 10.1016/j.jenvman.2022.114955.

Wang F., Zhao J., Miao H., Zhao J., Zhang H., Yuan J., Yan J., 2018. Current status and challenges of the ammonia escape inhibition technologies in ammonia-based CO$_2$ capture process. *Appl. Energy*, 230, 734–749. DOI: 10.1016/j.apenergy.2018.08.116.

Yang N., Yu H., Li L., Xu D., Han W., Feron P., 2014. Aqueous ammonia (NH$_3$) based post combustion CO$_2$ capture: A review. *Oil Gas Sci. Technol. – Rev. d'IFP Energies nouvelles*, 69, 931–945. DOI: 10.2516/ogst/2013160.

Zhang Q., Cheng C., Wu T., Xu G., Liu W., 2020. The effect of Fe$_3$O$_4$ nanoparticles on the mass transfer of CO$_2$ absorption into aqueous ammonia solutions. *Chem. Eng. Process. Process Intensif.*, 154, 108002. DOI: 10.1016/j.cep.2020.108002.